This full text paper was peer reviewed at the direction of IEEE Communications Society subject matter experts for publication in the WCNC 2010 proceedings.

Experimental Investigation of MIMO Relay Transmission Based on Wideband Outdoor Measurements at 2.35 GHz

Xin Nie*†, Jianhua Zhang*†, Zemin Liu*, Ping Zhang*†, Zhiyong Feng*
*Key Laboratory of Universal Wireless Communications, Ministry of Education
†Wireless Technology Innovation Institute
Beijing University of Posts and Telecommunications, P.O. box #92, China,100876
Email: niexin@mail.wtilabs.cn, jhzhang@bupt.edu.cn

***Abstract*—In order to obtain a more accurate assessment of relay performance in real-world outdoor propagation environment and to provide guidelines for the relay-based system deployment in the IMT-Advanced frequency band, the performance of a variety of relay schemes is investigated based on wideband measurements. The measurements were conducted at 2.35 GHz with 50 MHz bandwidth, which is within the frequency bands allocated to the IMT-Advanced system. We pay attention to two aspects: 1) the performance evaluation of a variety of transmission schemes in real propagation environment, and 2) the impact of propagation environment on the relay performance. Based on the measured channel transfer matrix, the achieved signal-to-noise ratio (SNR), spatial diversity and capacity of different transmission schemes are analyzed and compared. The measurement results reveal that in the NLOS region of the base station (BS) or in the region far away from the BS, the decode-and-forward (DF) relaying can significantly enhance the system performance. When the quality of the link between the BS and the relay station (RS) is good, the DF can provide larger performance improvement than the amplify-and-forward relaying. It is also found that propagation condition in the link between the RS and MS has major impact on the SNR, but minor impact on the spatial diversity.**

I. Introduction

The frequency band from 2.3 to 2.4 GHz was allocated for the IMT-Advanced systems by the World Radiocommunication Conference in 2007. As one of the most promising candidate technologies for the IMT-Advanced system, the relay has been attracting great attentions because of its various advantages over the conventional cellular system regarding the enhancement of coverage range, diversity, and achievable rates [1], [2]. The relay-based multiple-input multiple-output (MIMO) system typically comprises the base station (BS), the relay station(RS), and the mobile station (MS), each equipped with multiple antennas. The RS forwards the data received wirelessly from the BS to the MS, and vice versa. Thus, the relay channel consists of three links, namely, the link between the BS and the RS (BS→RS), the link between the RS and the MS (RS→MS), and the link between the BS and the MS (BS→MS).

Theoretical performance of the relay-based MIMO system has been analyzed in many literatures. However, most existing works were carried out under simplified assumptions for the channel properties [3], [4]. More details of the channel need to be included in the evaluation to get more accurate results. Measurement-based evaluations of the relay-based system performance were discussed by several researchers lately. In [5], [6], the rate improvement utilizing relay under real indoor propagation was investigated. The effect of relay location on channel capacity was reported in [7]. The achievable performance of relay system in real outdoor-to-indoor scenario was predicted in [8]. In [9], a real-time DSP-based testbed was constructed and BERs of cooperating relaying schemes were tested in indoor scenarios. However, most of the measurements were conducted in the indoor scenarios, measurement and analysis results of wideband outdoor relay channel are scarce. Besides, due to the limitation of indoor measurement site in the dimension, the changes of signal strength and capacity over space were left undiscussed. Moreover, the relay measurements conducted in IMT-Advance frequency bands were not reported in the previous works.

We conducted a measurement campaign at the center frequency of 2.35 GHz with 50 MHz bandwidth. The channel sounding for relay measurement consists of measurements of three individual links, i.e., the BS→MS link, the BS→RS link and the RS→MS link. The purpose of this paper is threefold: 1) to evaluate the performance of a variety of transmission schemes in real outdoor propagation environment, 2) to compare the performance of transmission schemes in different propagation conditions, 3) to investigate the impact of the propagation environment on the performance of the relay-based system.

The rest of this paper is organized as follows. Section II describes the measurement equipment and environment. Section III shows the procedure of data post-processing. Section IV lists the aspects of relay performance that we are interested in, including signal-to-noise ration (SNR), spatial diversity, and capacity. Calculation methods are also given. Section V compares and analyzes measurements results of three different transmission schemes, i.e., direct transmission (DT), amplify-and-forward (AF) and decode-and-forward (DF) relaying. Section VI summaries the conclusion of our work.

978-1-4244-6398-5/10/$26.00 ©2010 IEEE

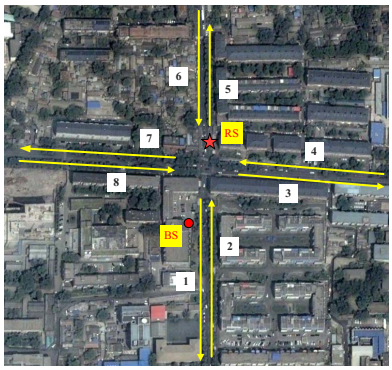

Fig. 1. Vertical view of measurement scenario. The circle mark indicates the position of the BS, while the star mark indicates the position of the RS. The straight links with arrow denote routes of MS, and the arrow shows the direction of MS movement.

II. Measurement

A. Equipment

The Elektrobit PropSound Channel Sounder was employed, which is described in more details in [10]. The sounder works in a time-division multiplexing mode. Periodic pseudo random binary signals (PRBS) are transmitted between different sub-channels. The interval within which all sub-channels are sounded once is referred to as a *measurement cycle*. The 3D cylinderal omni-directional array (ODA), which consists of 56 dual-polarized patch elements, was utilized at the BS, RS and MS. One ring of the elements were selected as the active antenna, i.e., 8 dual-polarized patch elements, which is the maximum antenna number considered in the IMT-Advanced system. The antenna pattern was obtained from Satimo SG128 antenna measurement system. Other important characteristics of measurement setup can be found in Table I.

B. Environment

The measurement was carried out in a typical urban area of Beijing, China. The measurement area is characterized by buildings ranging from 4 to 8 floors. The measurement scenario is illustrated in Fig. 1. During the measurement, the BS antennas were placed on the roof top of a 5-floor high building, which was about 22 m in height. Considering the relay antennas are typically lower than the BS antennas in order to reduce operating and maintenance costs [2], the RS antennas were placed on a testing vehicle around 7 m above the street. In addition, there is typically LOS existing between the BS and the RS to maximize the coverage [11], so the RS was placed in the LOS area of the BS. Antennas of the MS were mounted on a trolley. The height of MS antennas was adjusted to about 1.8 m in order to imitate the height of human body. By moving antennas of the MS, eight continuous routes were measured. The positions of MS were recorded by Global Positioning System. Both LOS and non-line-of-sight (NLOS) scenarios were measured. The description for propagation condition of every route in BS→MS and RS→MS link is given in Table II. The measurement routes are categorized into three subscenarios: 1) subscenarios I: the LOS exists in both BS→MS and RS→MS links, 2) subscenarios II: NLOS propagation is dominant in both BS→MS and RS→MS links, 3) subscenarios III: LOS exists in the RS→MS link, but the LOS is blocked in the BS→MS link.

TABLE I
Measurement Parameters

Items	Settings
Carrier Frequency (GHz)	2.35
Bandwidth (MHz)	50
Code length (chips)	255
Transmitting power (dBm)	26
Types of antennas	ODA
Number of BS antenna N_{BS}	8
Number of RS antenna N_{RS}	8
Number of MS antenna N_{MS}	8
Height of BS antenna (m)	22
Height of RS antenna (m)	7
Height of MS antenna (m)	1.8

TABLE II
Description of MS routes for LOS and NLOS cases

Route	BS→MS	RS→MS
#1-2	LOS	LOS
#3-4	NLOS	NLOS
#5-6	NLOS	LOS
#7-8	NLOS	NLOS

III. Data Post-Processing

Raw data collected by the receiver of channel sounder are the spread signals with the system impulse response of the sounding system. Raw data are cyclically correlated with the system impulse response, which is obtained from the calibration of the sounder, to remove the effect of the sounding system. Then, channel impulse responses (CIRs), i.e. $h(t,\tau)$, are calculated through the cyclic correlation with the known PRBS.

Since the noise level P_n is subjected to the measurement environments and varies with time, the noise level estimation is done for each measurement cycle. To ensure that the signal is much stronger than the noise so that the additive noise does not affect the inherent characteristic of the channel, a threshold P_t is then determined by both the estimated noise level P_n and the peak power of CIRs P_p,

$$P_t = \max\{P_n + D_m, P_p - D_r\}, \tag{1}$$

where D_m is the noise margin from noise floor P_n and D_r denotes the dynamic range from the peak power P_p. Paths with power $|h(t,\tau)|^2$ below the threshold P_t are ignored. The dynamic range D_r is set to 25 dB and the margin D_m is set to 6 dB. After the noise-cut, the corresponding frequency transfer functions $\mathbf{H}(t,f)$ can be obtained via the Fourier transform. Assuming that the $\mathbf{H}(j,k)$ is the sample of $\mathbf{H}(t,f)$, we get

$$\mathbf{H}(j,k) = \mathbf{H}(t,f)|_{t=j\cdot\Delta t, f=k\cdot\Delta f} = \mathbf{H}(j\cdot\Delta t, k\cdot\Delta f) \tag{2}$$

where Δt and Δf are the sampling intervals in the time and frequency domain, respectively.

IV. Performance Evaluation Based on Measured Channels

A time domain duplex relay protocol is chosen for comparison among different relaying schemes. In order to complete the data transmission, two consecutive time slots are required in the protocol. In the first time slot, the source broadcasts signals to the relay and destination. Afterwards, the relay communicates with the destination in the second time slot. In AF relaying scheme, the relay amplifies the received signal from the source and transmits it to the destination in the next time slot. The relay retransmits the decoded signal to the destination after receiving signals from the source in the previous time slot in the DF scheme. In both relaying schemes, the signals received from the BS→MS and the BS→RS→MS are summed using Maximal Ratio combining (MRC).

For a fair comparison, the transmitting power of the BS and RS, i.e., P_{BS} and P_{RS}, are allocated under the constraint that $P_{BS} + P_{RS} = P_0$. In our analysis, equal power allocation is assumed, namely, $P_{BS} = P_{RS} = P_0/2$. The DT is considered as a baseline for comparison. Since only one time slot is required in DT, the source can use the first and second time slot to transmit different data with the transmitted power $P_0/2$. Let $\boldsymbol{n}_0$ be the noise vector at the MS in the BS→MS link, $\boldsymbol{n}_1$ be the noise vector at the RS in the BS→RS link, and $\boldsymbol{n}_2$ be the noise vector at the MS in the RS→MS link. We assume the noises at all receivers have equal variance, namely, $\mathcal{E}\{\boldsymbol{n}_0\boldsymbol{n}_0^\dagger\} = \mathcal{E}\{\boldsymbol{n}_2\boldsymbol{n}_2^\dagger\} = \mathbf{R}_2 = \sigma^2\mathbf{I}_{N_{\rm MS}}$ and $\mathcal{E}\{\boldsymbol{n}_1\boldsymbol{n}_1^\dagger\} = \mathbf{R}_1 = \sigma^2\mathbf{I}_{N_{\rm RS}}$. Based on the $N_{\rm MS} \times N_{\rm BS}$ matrix $\mathbf{H}_0$, $N_{\rm RS} \times N_{\rm BS}$ matrix $\mathbf{H}_1$ and $N_{\rm MS} \times N_{\rm RS}$ matrix $\mathbf{H}_2$, which are the channel transfer matrices (CTMs) of BS→MS, BS→RS, and RS→MS links, respectively, the performance of DT, AF and DF relaying schemes are investigated.

A. Signal-to-noise Ratio

The effect of slow fading is removed by taking the sliding mean of the sequence of the measured CTMs by

$$\|\mathbf{H}^{avr}(j,k)\|_{\mathcal{F}}^2 = \frac{1}{2N_{sw}+1}\sum_{j-N_{sw}}^{j+N_{sw}} \|\mathbf{H}(j,k)\|_{\mathcal{F}}^2, \quad (3)$$

where the superscript avr refers to the sliding mean and $\|\cdot\|_{\mathcal{F}}$ denotes the Frobenius-norm. The length of the sliding window is $2N_{sw}+1$. The N_{sw} is selected having the value of 100 such that the measured CTMs in one sliding window are in a local area, the radius of which is 20 times of the wavelength.

1) Direct transmission: In the case of DT, the SNR can be calculated using as

$$\gamma_{DT} = \gamma_0 = \frac{P_0\,\|\mathbf{H}_0\|_{\mathcal{F}}^2}{2\sigma^2}. \quad (4)$$

2) AF relaying scheme: Using the results in [12], the overall SNR at the MS after MRC can be obtained as

$$\gamma_{AF} = \gamma_0 + \frac{\gamma_1\gamma_2}{\gamma_1+\gamma_2+1}, \quad (5)$$

where $\gamma_0 = \frac{P_0\|\mathbf{H}_0\|_{\mathcal{F}}^2}{2\sigma^2}$, $\gamma_1 = \frac{P_0\|\mathbf{H}_1\|_{\mathcal{F}}^2}{2\sigma^2}$ and $\gamma_2 = \frac{P_0\|\mathbf{H}_2\|_{\mathcal{F}}^2}{2\sigma^2}$ are the SNRs of the BS→MS, BS→RS and RS→MS, respectively.

3) DF relaying scheme: For the DF relaying scheme, the SNR at the MS is determined by the SNRs of three links, namely,

$$\gamma_{DF} = \min\{\gamma_1, \gamma_0+\gamma_2\}. \quad (6)$$

B. Spatial Diversity

The spatial diversity of a MIMO channel is specified by the *eigenvalues*, which define the number of independently fading components and their associated power. The number of significant eigenvalues determines the maximum degree of diversity and the principle eigenvalues specify the maximum possible beamforming gain. Hence, we choose the marginal cumulative distribution function (CDF) of each ordered eigenvalue as the spatial diversity metric. Let $\lambda_{r,i,j}, r = 1,2,\ldots,R$, be the eigenvalues of $\mathbf{H}(j,k)\mathbf{H}(j,k)^\dagger$ in descending order, i.e.,

$$\lambda_{1,i,j} \geq \lambda_{2,i,j} \ldots \lambda_{R,i,j} \geq 0, \quad (7)$$

where $R = \text{rank}\left\{\mathbf{H}(j,k)\mathbf{H}(j,k)^\dagger\right\}$.

1) Direct transmission: In the case of DT, the eigenvalues can be obtained after the singular value decomposition (SVD) on $\mathbf{H}_0$.

2) AF relaying scheme: For the AF relaying scheme, the overall received signals at the MS can be written as

$$\boldsymbol{y} = \begin{bmatrix} \mathbf{H}_0 \\ \mathbf{H}_2\mathbf{G}\mathbf{H}_1 \end{bmatrix}\boldsymbol{x} + \begin{bmatrix} \boldsymbol{n}_0 \\ \mathbf{H}_2\mathbf{G}\boldsymbol{n}_1 + \boldsymbol{n}_2 \end{bmatrix}, \quad (8)$$

Thus, the compound CTM $\mathbf{H}_{AF}$ from the BS to the MS can be expressed as $\mathbf{H}_{AF} = [\mathbf{H}_0 \quad \mathbf{H}_2\mathbf{G}\mathbf{H}_1]^T$.

3) DF relaying scheme: Since the propagation condition in the BS→RS link is good, the perfect decoding at the RS is assumed. The received signals at the MS in the case of DF relaying scheme is,

$$\boldsymbol{y} = \begin{bmatrix} \mathbf{H}_0 \\ \mathbf{H}_2 \end{bmatrix}\boldsymbol{x} + \begin{bmatrix} \boldsymbol{n}_0 \\ \boldsymbol{n}_2 \end{bmatrix}, \quad (9)$$

then, the compound CTM from the BS to the MS, i.e., $\mathbf{H}_{DF}$, yields $\mathbf{H}_{DF} = [\mathbf{H}_0 \quad \mathbf{H}_2]^T$. The eigenvalues can be got after the SVD operation on the compound CTMs, i.e., $\mathbf{H}_{AF}$ and $\mathbf{H}_{DF}$.

C. Capacity

Capacity enhancement is the main benefit resulted from applying MIMO for spatial multiplexing. It is not fair to compare the channel capacity at the premise that all channel realizations are normalized to have the same channel gain [13], [14]. In our analysis, to preserve the effect of large scale fading, the difference in channel gain of the measured CTMs are retained.

1) Direct transmission: The channel capacity of DT can be calculated as [15]

$$C_{DT}(t) = \frac{1}{B}\int \log_2\det\Big(\mathbf{I} + \frac{\rho}{N_{\rm Tx}}\mathbf{H}_0(t,f)\mathbf{H}_0^\dagger(t,f)\Big)df, \quad (10)$$

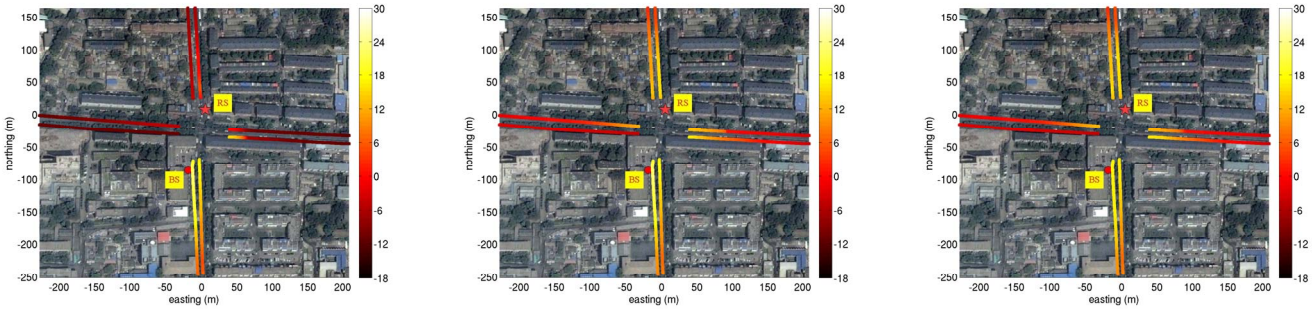

(a) Average SNR of different routes for the DT. (b) Average SNR of different routes for the AF. (c) Average SNR of different routes for the DF.

Fig. 2. Average SNR for different routes.

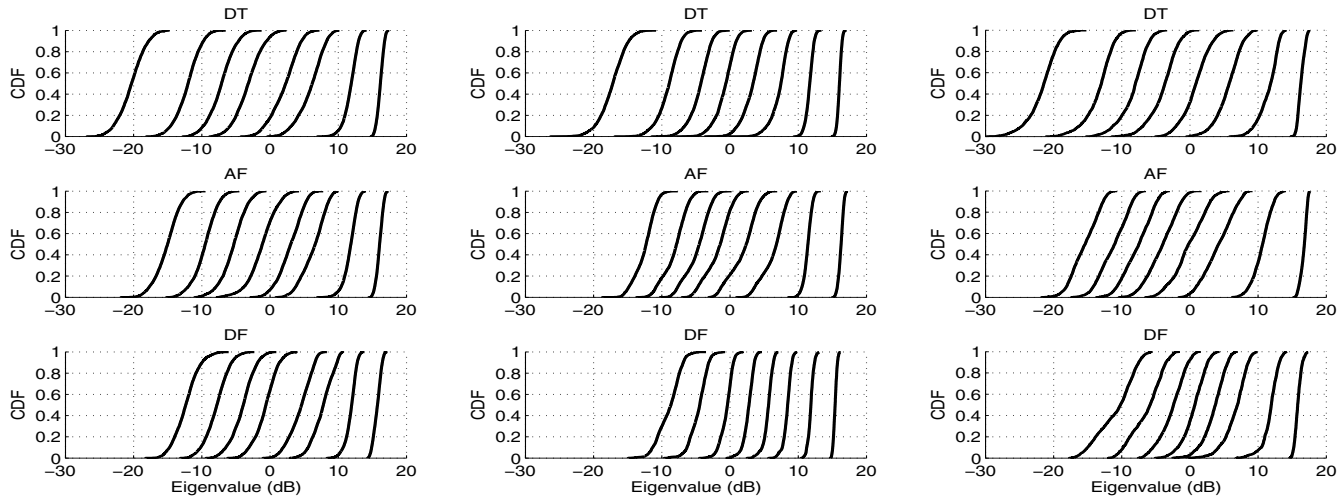

(a) CDFs of eigenvalues in subscenario I. (b) CDFs of eigenvalues in subscenario II. (c) CDFs of eigenvalues in subscenario III.

Fig. 3. CDFs of eigenvalues for three cases. For each subfigure: Top: the eigenvalues for the DT. Middle: the eigenvalues for the AF. Bottom: the eigenvalues for the DF.

where B is the bandwidth and N_{Tx} is the number of transmitter antennas. For the discrete channel $\mathbf{H}(j,k)$, an approximation can be given by

$$C_{DT}(j) \approx \frac{1}{K}\sum_{k=1}^{K}\log_2\det\Big(\mathbf{I}+\frac{\rho}{N_{\mathrm{Tx}}}\mathbf{H}_0(j,k)\mathbf{H}_0^{\dagger}(j,k)\Big), \quad (11)$$

where K is the number of the frequency bins. For simplicity, the transmitted power is assumed to be allocated equally over all the antennas.

2) AF relaying scheme: The capacity of kth frequency bin in AF relaying scheme can be calculated as below [16],

$$C_{AF}(k) = \frac{1}{2}\log_2\det\left(\mathbf{I}_{2N_{\mathrm{MS}}} + \mathbf{R}_0^{-1}\mathbf{H}_{AF}\mathbf{Q}\mathbf{H}_{AF}^{\dagger}\right), \quad (12)$$

where

$$\mathbf{R}_0 = \sigma^2\begin{bmatrix} \mathbf{I}_{N_{\mathrm{MS}}} & \mathbf{0} \\ \mathbf{0} & \mathbf{I}_{N_{\mathrm{MS}}} + \mathbf{H}_2\mathbf{G}\mathbf{G}^{\dagger}\mathbf{H}_2^{\dagger}, \end{bmatrix} \quad (13)$$

and $\mathbf{Q} = \mathcal{E}\{\boldsymbol{x}\boldsymbol{x}^{\dagger}\}$. When the power is equally allocated to antennas of the BS, $\mathbf{Q} = (P_0/2N_{\mathrm{BS}})\,\mathbf{I}_{N_{\mathrm{MS}}}$. $\mathbf{G}$ is the amplification matrix with the diagonal element g equaling to

$$g = \sqrt{\frac{P_0 N_{\mathrm{BS}}}{P_0\|\mathbf{H}_1\|_{\mathcal{F}}^2 + 2N_{\mathrm{BS}}N_{\mathrm{RS}}\sigma^2}}. \quad (14)$$

With the amplification matrix $\mathbf{G}$ given by (14), the total transmitted power in two time slots is restricted to P_0. Then, the C_{AF} can be obtained as

$$C_{AF} = \frac{1}{K}\sum_{k=1}^{K} C_{AF}(k), \quad (15)$$

where the factor $1/2$ is due to the half-duplex transmission.

3) DF relaying scheme: The end-to-end system performance of DF relaying is mainly dominated by characteristics of the link with worse performance, thus, the capacity can be

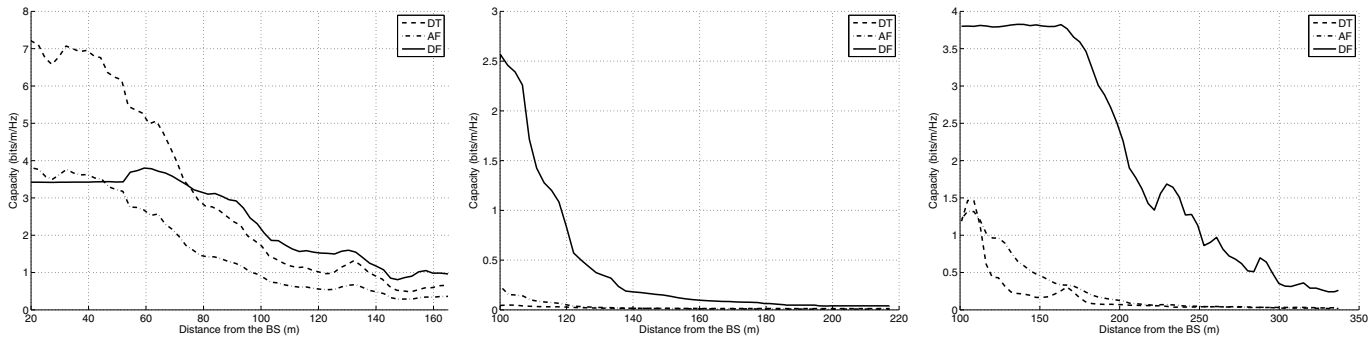

(a) End-to-end capacity in the subscenario I. (b) End-to-end capacity in the subscenario II. (c) End-to-end capacity in the subscenario III.

Fig. 4. End-to-end capacity in different subscenarios.

obtained as

$$C_{DF} = \frac{1}{2}\min\{C_{DF}^{1}, C_{DF}^{02}\}, \tag{16}$$

where C_{DF}^{1} is the capacity of the BS→RS,

$$C_{DF}^{1} = \log_2 \det\left(\mathbf{I} + \mathbf{R}_1^{-1}\mathbf{H}_1\mathbf{Q}\mathbf{H}_1^{\dagger}\right), \tag{17}$$

and

$$C_{DF}^{02} = \log_2 \det\left(\mathbf{I} + \mathbf{R}_2^{-1}\mathbf{H}_{DF}\mathbf{Q}\mathbf{H}_{DF}^{\dagger}\right). \tag{18}$$

V. Measured Results and Analysis

A. Signal-to-noise Ratio

The SNRs of all measurement routes as a function of MS position relative to the BS are shown in Fig. 2. Colors represent SNR in dB. Fig. 2(a) gives the SNRs when the DT is adopted. The SNRs range from -18 to 30 dB. The SNRs in LOS region (routes #1 and #2) are significantly larger than those in NLOS region. The maximum difference is 48 dB. Besides, compared to other NLOS routes, the SNRs of route #5 and #6 are higher, which is mainly due to the waveguide effect of street canyon. The SNRs for AF and DF are given in Fig. 2(b) and 2(c), respectively. The RS provides a better coverage in the NLOS part of the BS, especially in the subscenario II, i.e., route #3, #4, #7 and #8. The SNRs are increased by an average of 15 dB. In the subscenario III, the improvement is about 10 dB.

B. Spatial Diversity

The CDFs of eight ordered eigenvalues for different transmission schemes are shown in Fig. 3. Rich scatterers tend to produce more even eigenvalues, thus provide higher diversiy/multiplexing gain. From the comparison of the same transmission scheme in different subscenarios, it can be observed that the eigenvalues in subscenarios II and III are more uniform than those in subscenario I. In the same subscenario, the DF introduces the most uniform eigenvalues. The AF takes the second place. This is mainly due to the difference in the equivalent CTMs of the AF and DF. The additional part of CTM provided by the AF and DF are $\mathbf{H}_2\mathbf{G}\mathbf{H}_1$ and $\mathbf{H}_2$, respectively. According to the matrix theory [17], we have

$$\operatorname{rank}\{\mathbf{AB}\} \leq \min\{\operatorname{rank}\{\mathbf{A}\}, \operatorname{rank}\{\mathbf{B}\}\}, \tag{19}$$

so that $\operatorname{rank}\{\mathbf{H}_2\mathbf{G}\mathbf{H}_1\} \leq \min\{\operatorname{rank}\{\mathbf{H}_0\}, \operatorname{rank}\{\mathbf{H}_2\}\}$. Thus, the diversity enhancement provided by the DF is larger than that provided by the AF. It can also be observed that when the LOS is blocked in the BS→MS link (MS moves from subsecnario I to subscenario III), the eigenvalues undergo greater changes than when the LOS is absent in the RS→MS link (MS moves from subsecnario III to subscenario II). These results indicate that the propagation condition in the BS→MS link have a larger impact on the spatial diversity than that in the RS→MS link. The observation can be attributed to the lower antenna height of the RS. Both the RS and the MS are surrounded by local scatterers, hence, there are enough scatterers to constitute a rich-scattering link even with the LOS propagation. Therefore, whether the LOS exists in the RS→MS link has minor impact on the spatial diversity.

C. Capacity

The capacity values as a function of the distance to the BS in three subscenarios are given in Fig. 4(a), 4(b) and 4(c). In subscenario I, when the MS is near the BS (the distance from the MS to the BS is less than 52 m), the DT provides the highest capacity (about 7 bits/s/Hz). Since when the MS is close to the BS, the signal transmitting from the direct link is much stronger than the signal forwarded by the relay. The capacity is mainly contributed by the $\mathbf{H}_0$. One time slot is required by the DT to complete the transmission, meanwhile, the AF and DF need two time slots. Thus, the capacity provided by the AF and DF is about 3.5 bits/s/Hz, which is 50 percents of the capacity provided by the DT. As the MS moves away from the BS, the signal arriving at the MS from the direct link weakens, and the contribution of $\mathbf{H}_0$ to the capacity decreases. Compared to the DT, the DF can provide extra spatial diversity. Thus, when the distance from the MS to the BS is more than 76 m, the capacity of the DF exceeds that of the DT. It can also be found that when the MS is in the near region of the BS, the AF can provide similar capacity as the DF. However, when the distance is larger than 60 m, a difference of 1.2 bit/s/Hz arises.

In subscenario II, the LOS between the BS and the RS is blocked, so the capacity provided by the DT significantly

decreases. The DF provides larger capacity than the DT. When the distance is 100 m, the capacity gap between the DF and the DT is 2.5 bits/s/Hz. As the distance increases, the gap decreases. When the distance reaches 150 m, the gap reduces to 0.2 bits/s/Hz. In subscenario III, the gap is 2.6 bits/s/Hz when the distance is 100 m. Even when the distance increases to 250 m, the gap remains above 1 bits/s/Hz. These results validate that the DF can enhance the capacity in the NLOS regions of the BS or the remote regions from the BS. It can also be seen that the capacity improvement brought by the AF is not as significant as the DF. The DF outperforms the AF in all three subscenarios. Since the AF and the DF can offer almost the same SNR improvement (see Fig. 2(b) and 2(c)), we ascribe the capacity difference to the difference between the spatial diversity brought by the AF and by the DF.

VI. Conclusion

In this paper, the performance of three transmission schemes, namely, the DT, AF and DF are assessed under the real outdoor propagation environment. The measurement area is divided into three subscenarios according to whether the LOS exists in the BS→MS and RS→MS link. We lay our emphasis on the SNR, spatial diversity, and capacity. Measurement results show that both the AF and DF can bring the SNR improvement, thus provide better coverage. The SNR improvement brought by the AF and DF are almost the same. In the subscenario II, the average SNR improvement is about 15 dB, and in the subscenario III, the improvement is about 10 dB. Then, The spatial diversity of transmission schemes in three subscenarios are compared. It is found that the DF can enhancement the diversity significantly. However, in the case of the AF, since the rank of the compound channel $\mathbf{H}_{AF}$ is under the constraint of the $\mathbf{H}_1$ and $\mathbf{H}_2$, the diversity enhancement is not as significant as the DF. Finally, the capacity values of three transmission schemes are given. The measured results reveal that in the LOS region, when the MS is near the BS, the DT provides the largest capacity. The AF and DF only provide 50 percents of capacity of the DT. As the distance increases, the signals transmitting from the direct link weakens. The capacity provided by the DF exceeds that provided by the DT. When the MS is in the NLOS region or far away from the BS, the DF can significantly improve the capacity. Different from the results reported in [8], the DF outperforms the AF in all subscenarios in our measurement. Since the AF and DF can offer almost the same SNR improvement, we ascribe the capacity difference to the difference between the spatial diversity brought by the AF and by the DF.

The impact of the propagation environment on the system performance is also discussed in this paper. Our measurement results reveal that the spatial diversity is mainly decided by the propagation condition in the BS→MS link. Due to the lower height of the RS antennas, both the RS and the MS are surrounded by local scatterers, hence, there are enough scatterers to constitute a rich-scattering link even with the LOS propagation. So whether the LOS exists in the RS→MS link has major impact on the SNR, but minor impact on the spatial diversity.

Acknowledgment

The research is supported in part by China Important National Science and Technology Specific Projects under Grant No. 2009ZX03007-003 and China 863 Program and Major Project name under Grant NO. 2009AA011502.

References

[1] A. Nosratinia, T. Hunter, and A. Hedayat, "Cooperative communication in wireless networks," *IEEE Commun. Mag.*, vol. 42, no. 10, pp. 74–80, 2004.

[2] R. Pabst, B. Walke, D. Schultz, P. Herhold, H. Yanikomeroglu, S. Mukherjee, H. Viswanathan, M. Lott, W. Zirwas, M. Dohler, H. Aghvami, D. Falconer, and G. Fettweis, "Relay-based deployment concepts for wireless and mobile broadband radio," *IEEE Commun. Mag.*, vol. 42, no. 9, pp. 80–89, 2004.

[3] J. Laneman, G. Wornell, and D. Tse, "An efficient protocol for realizing cooperative diversity in wireless networks," in *Proc. IEEE International Symposium on Information Theory 2001 (ISIT'01)*, 24–29 June 2001, p. 294.

[4] R. Nabar, H. Bolcskei, and F. Kneubuhler, "Fading relay channels: performance limits and space-time signal design," *IEEE J. Sel. Areas Commun.*, vol. 22, no. 6, pp. 1099–1109, Aug. 2004.

[5] P. Kyritsi, P. Eggers, R. Gall, and J. Lourenco, "Measurement based investigation of cooperative relaying," in *Proc. IEEE 64th Vehicular Technology Conference (VTC'06-Fall)*, 2006, pp. 1–5.

[6] P. Kyritsi, P. Popovski, P. Eggers, Y. Wang, D. Khan, A.-E. Bouaziz, B. Pietrarca, and G. Sasso, "Cooperative transmission: a reality check using experimental data," in *Proc. IEEE 65th Vehicular Technology Conference (VTC'07-Spring)*, 2007, pp. 2281–2285.

[7] L. Jiang, L. Thiele, and V. Jungnickel, "Modeling and measurement of MIMO relay channels," in *Proc. IEEE 67th Vehicular Technology Conference (VTC'08-Spring)*, 2008, pp. 419–423.

[8] K. Haneda, V.-M. Kolmonen, T. Riihonen, R. Wichman, P. Vainikainen, and J. Takada, "Evaluation of relay transmission in outdoor-to-indoor propagation channels," in *Proc. COST2100 2nd Workshop on MIMO and Cooperative Communications*, 2008.

[9] Per Zetterberg, Christos Mavrokefalidis, Aris S. Lalos, and Emmanouil Matigakis, "Experimental investigation of cooperative schemes on a real-time DSP-based testbed," *EURASIP Journal on Wireless Communications and Networking*, vol. 2009, Article ID 368752, 15 pages, 2009. doi:10.1155/2009/368752.

[10] Elektrobit, "Propsound multidimensional channel sounder." [Online]. Available: http://www.propsim.com

[11] M. Herdin, "MIMO amplify-and-forward relaying in correlated MIMO channels," in *Proc. 15th International Conference on Information, Communications and Signal Processing*, 2005, pp. 796–800.

[12] A. Agustin, "Relay-assisted transmission and radio resource management for wireless networks," Ph.D. dissertation, 2008. [Online]. Available: http://www.tesisenxarxa.net/tesis_upc/available/tdx-0701108-121341

[13] T. Svantesson and J. Wallace, "On signal strength and multipath richness in multi-input multi-output systems," in *Proc. IEEE International Conference on Communications 2003 (ICC'03)*, vol. 4, 11–15 May 2003, pp. 2683–2687.

[14] H. Nishimoto, Y. Ogawa, T. Nishimura, and T. Ohgane, "Measurement-based performance evaluation of MIMO spatial multiplexing in a multipath-rich indoor environment," *IEEE Trans. Antennas Propag.*, vol. 55, no. 12, pp. 3677–3689, 2007.

[15] A. Paulraj, R. Nabar, and D. Gore, *Introduction to Space-Time Wireless Communications*. Cambridge University Press, 2003.

[16] O. Munoz, J. Vidal, and A. Agustin, "Non-regenerative MIMO relaying with channel state information," in *Proc. IEEE International Conference on Acoustics, Speech, and Signal Processing (ICASSP'05)*, vol. 3, 2005, pp. iii/361–iii/364 Vol. 3.

[17] R. Horn and C. Johnson, *Matrix Analysis*. Cambridge University Press, 1990.